Published in final edited form as:
J Comp Neurol. 2014 May 1; 522(7): 1527–1541. doi:10.1002/cne.23479.

Age-Related Neurochemical Changes in the Rhesus Macaque Cochlear Nucleus

Daniel T. Gray[1], **James R. Engle**[2], and **Gregg H. Recanzone**[1,3,*]

[1]Center for Neuroscience, University of California at Davis, Davis, CA 95616

[2]Evelyn F. McKnight Brain Institute, University of Arizona, Tucson, AZ 85721

[3]Department of Neurobiology, Physiology and Behavior, University of California at Davis, Davis, CA 95616

Abstract

Neurochemical changes in the expression of various proteins within the central auditory system have been associated with natural aging. These changes may compensate in part for the loss of auditory sensitivity arising from two phenomena of the aging auditory system: cochlear histopathologies and increased excitability of central auditory neurons. Recent studies in the macaque monkey have revealed age-related changes in the density of nicotinamide adenine dinucleotide phosphate (NADPH)-diaphorase (NADPHd) and parvalbumin (PV)-positive cells within the inferior colliculus and superior olivary complex. The cochlear nucleus (CN), which is the first central auditory nucleus, remains unstudied. Since the CN participates in the generation of the auditory brainstem response (ABR) and receives direct innervation from the cochlea, it serves as an ideal nucleus to compare the relationship between these neurochemical changes and the physiological and peripheral changes of the aging auditory system. We used stereological sampling to calculate the densities of NADPHd and PV reactive neurons within the three subdivisions of the CN in middle-aged and aged rhesus macaques. Regression analyses of these values with ABR properties and cochlear histopathologies revealed relationships between these cell types and the changing characteristics of the aging auditory system. Our results indicate that NADPHd expression does change with age in a specific subdivision of the CN, but PV does not. Conversely, PV expression correlated with ABR amplitudes and outer hair cell loss in the cochlea, but NADPHd did not. These results indicate that NADPHd and PV may take part in distinct compensatory efforts of the aging auditory system.

*CORRESPONDENCE TO: Gregg H. Recanzone, Center for Neuroscience, 1544 Newton Ct., Davis, CA 95618. ghrecanzone@ucdavis.edu.

CONFLICTS OF INTEREST

The authors claim no conflicts of interest.

ROLE OF AUTHORS

All authors had full access to all the data in the study and take responsibility for the integrity of the data and the accuracy of the data analysis. Study concept and design: DTG, JRE, GHR. Acquisition of data: DTG, JRE. Analysis and interpretation of data: DTG, GHR. Drafting of the article: DTG, GHR. Critical revision of the article for important intellectual content: DTG, GHR. Statistical analysis: DTG. Obtained funding: JRE, GHR. Administrative, technical, and material support: DTG, JRE. Study supervision: GHR.

INDEXING TERMS

NADPH-diaphorase; parvalbumin; brainstem; ABR; monkey; geriatric; aging

The mammalian central auditory system is segregated into chemically distinct parallel processing pathways originating at the level of the cochlear nucleus (CN), and terminating in the primary auditory cortex (Jones, 2003; Loftus et al., 2008). Two chemical markers common to these processing streams are the nitric oxide synthase nicotinamide adenine dinucleotide phosphate (NADPH)-diaphorase (NADPHd) and the calcium-binding protein parvalbumin (PV). The relative densities of neurons expressing these proteins change with natural aging in the auditory structures of rodents, carnivores, and nonhuman primates (Zettel et al., 1997; Reuss et al., 2000; Ouda et al., 2003, 2008; Sanchez-Zuriaga et al., 2007; Huh et al., 2008; Gray et al., 2013a), and consequently these changes are thought to relate to age-related structural and physiological changes of the aging auditory system. The primary processing deficits characteristic of age-related hearing loss manifest as a consequence of either structural insults in the periphery (Hawkins et al., 1986; Fetoni et al., 2011; Engle et al., 2012), age-related decreases in central inhibition leading to more excitable auditory neurons (Caspary et al., 1995, 1999, 2008), or both. Therefore, the age-related changes in the expression of NADPHd+ and PV+ neurons may help compensate for the decreased output of the auditory periphery and/or the changes in neural excitability. If the age-related increases of these two neural markers are in fact compensatory, they may act upon different pathologies since their physiological actions differ substantially within the central nervous system (Esplugues, 2002; Rudy et al., 2010).

PV acts as one of several calcium-binding proteins in the central nervous system. Several processes such as neurotransmitter release, maintenance of cytoarchitecture, plasticity, and memory formation are at least in part calcium-dependent (Disterhoft et al., 1995; Toescu and Vreugdenhil, 2010; Tang et al., 2011), and show age-related changes. Hence, understanding changes in calcium-dependent processes has proven important in understanding the aging nervous system. Staining for proteins such as PV gives indirect insight into some of these calcium dependent processes and allows for simple quantifications of age-related changes. The auditory system has been extensively studied in this manner, and changes in the density of neurons expressing these calcium-binding proteins has been repeatedly shown in the auditory system of aged animals (Zettel et al., 1997; Ouda et al., 2008, Gray et al., 2013a).

The actions of many enzymes are calcium-dependent, and therefore also show age-related changes. For example, the nitric oxide synthase NADPHd relies on the high calcium environment surrounding N-methyl-D-aspartate (NMDA) receptors to produce nitric oxide (NO; Bredt and Snyder 1990; Brenman et al., 1996; Fessenden and Schacht, 1998). NO diffuses from the cell and acts primarily as a signaling molecule and neuromodulator. NADPHd is found throughout the nervous system (reviewed by Esplugues, 2002; Hopper, 2004) and extensively throughout the auditory system; however, its primary role in audition remains unclear. Nevertheless age-related changes in NADPHd density have been shown several times in both rodents and primates (Reuss et al., 2000; Ouda et al., 2003; Sanchez-

Zuriaga et al., 2007; Huh et al., 2008; Gray et al., 2013a), and thus likely plays a role in the aging process.

In the macaque, age-related processing declines and histopathologies have been noted, and in most cases high-frequency hearing ability appears to be most affected. For example, aged macaques experience increases in their audiometric thresholds measured both psychophysically and with the auditory brainstem response (ABR), with an exaggeration in high-frequency hearing loss (Bennet et al., 1983; Torre and Fowler, 2000; Navarro et al., 2008; Engle et al., 2012). Distortion product OAEs decrease with age at all frequencies, and this change is also exaggerated for high-frequency stimuli (Torre and Fowler, 2000). Furthermore, the basal (high frequency) region of the aged cochlea experiences the greatest loss of outer hair cells and spiral ganglion cells (Engle et al., 2012). Some of these physiological and anatomical metrics correlate along the ascending auditory system of primates. For example, across age groups ABR amplitudes to clicks and high-frequency tones significantly correlate with NADPHd- and PV-immunoreactive cell densities within specific subdivisions of the superior olivary complex (SOC; Gray et al., 2013a) and inferior colliculus (unpubl. obs.), suggesting involvement of these cell types in age-related changes of central auditory processing.

The chemical changes in these brainstem and midbrain auditory structures suggests that the macaque's central auditory system alters the expression of these cell classes beginning at least at the level of the SOC. Furthermore, the correlations between these changes and ABR amplitudes in both the SOC and IC suggest that these cell types are related to physiological responses in some capacity along the ascending auditory system. What remains unclear is whether these age-related changes are initiated in the SOC or in a lower region that provides input to the SOC, the cochlear nucleus.

The CN is the first major nucleus of the central auditory system, yet to our knowledge is unstudied with regard to age-related neurochemical changes in the macaque. Two distinct bifurcations of the auditory nerve create the three subdivisions of the CN, the dorsal cochlear nucleus (DCN) and the anterior (AVCN) and posterior (PVCN) divisions of the ventral cochlear nucleus. Hence, the histopathological changes in the cochlea directly affect the CN, since spiral ganglion cells innervate this nucleus.

The AVCN and PVCN provide the majority of input to the SOC, and the DCN projects directly to the central nucleus of the IC. Both the SOC and IC have shown age-related histopathologies that correlate with physiological responses of the auditory brainstem. Therefore, the CN likely does as well, and furthermore it is an ideal nucleus to compare how age-related neurochemical changes relate to structural insults in the periphery and the physiological changes characteristic of the aging auditory system, and specifically which proteins relate most to which pathology. Therefore, age-related changes in NADPHd and PV neuronal densities and the relationship of these densities with ABRs and cochlear histopathologies were investigated in all three subdivisions of the macaque CN.

MATERIALS AND METHODS

The CN from eight rhesus macaques ranging from middle to old age (12 to 35 years of age, corresponding roughly to 36 to 105 human years; Davis and Leathers, 1985) were examined and quantified for NADPHd and PV reactivity using unbiased stereological sampling techniques. Detailed methods can be found in Gray et al. (2013a).

Animals

The demographic information for all monkeys used in this study is shown in Table 1. These animals were the same as those used in characterizations of the SOC (Gray et al., 2013a) with the exception that one young animal (184 months) from that study was replaced by another young animal (245 months) in the present study. Furthermore, the cochleae from five of these animals were used in a study characterizing various age-related histopathologies of the aged cochlea (Engle et al., 2012), and these data were used in the analysis described below. The inclusion criteria for the animals were: 1) no history of ototoxic drug treatment; 2) no history of loud noise exposure or ear trauma; and 3) no outer ear occlusions or otitis media. The animals were maintained on ad libitum food and had free access to water. All procedures adhered to the National Institutes of Health guidelines for animal use and were approved by the UC Davis Institutional Animal Care and Use Committee.

ABR procedure

ABRs were recorded from all monkeys except for the 12-year-old. The animals were anesthetized with ketamine (10 mg/kg, IM) and medatomidine (.3 ml/10 kg, IM) with supplemental doses of ketamine administered as needed throughout the procedure to maintain an appropriate level of chemical restraint. The animals were placed in the prone position with their heads slightly elevated within an electrically and acoustically quiet room or a double-walled acoustic chamber (depending on the housing location of the animals). There was no difference in recording quality noted between conditions. The skin was cleaned with alcohol and sterile 0.22G stainless steel skin electrodes were placed subcutaneously behind both ears, on the forehead, and on the back of the neck (Allen and Starr, 1978; Torre and Fowler, 2000; Torre et al., 2004; Fowler et al., 2010). ABRs were collected using an Intelligent Hearing System (Smart EP Win USB, v. 3.97) controlled by a laptop PC (Dell). Auditory stimuli consisted of clicks and 10 ms (2 ms trapezoidal rise/fall) tone bursts (0.5, 1, 2, 4, 8, 12, and 16 kHz) presented via ear buds at a rate of 10 stimuli/sec. Each stimulus was repeated a minimum of 1,000 times to obtain reliable average ABR recordings. The stimuli were first presented at 80 dB SPL, and then decreased by 10 dB increments until a clearly responsive ABR peak II and peak IV was absent. The intensity was then increased by 5 dB to determine whether the waveform would return. Therefore, the values that did and did not evoke an ABR waveform were always separated by 5 dB, and threshold was determined to be the arithmetic mean of these two values.

Two independent observers analyzed and scored the amplitudes and latencies of ABR waveforms with an interobserver agreement of 95% or greater. In accordance with previous studies (Laughlin et al., 1999; Navarro et al., 2008), amplitude was defined as the evoked

potential from the summit of the peak to the lowest point of the ensuing trough, and latency was defined as the time from stimulus presentation to the summit of the peak. In our hands, wave II was the most reliable waveform to which the CN is thought to contribute (Møller and Burgess, 1986); therefore, we only used this wave in subsequent analyses.

Histological processing and antibody characterization

Histological procedures were identical to those previously described (Gray et al., 2013a). Briefly, the animals were euthanized with a lethal dose of sodium pentobarbital (60 mg/kg, IV) and transcardially perfused with saline, a mixture of 4% paraformaldehyde and 0.1% glutaraldehyde in 0.1% phosphate buffer (pH 7.4), and a mixture of 4% paraformaldehyde and 10% sucrose. The brains were extracted and cryoprotected in a mixture of 4% paraformaldehyde and 30% sucrose. All eight brains were cut perpendicular to the lateral sulcus at thicknesses ranging from 25–50 μm. The tissue was washed and stored in 0.1% phosphate buffer prior to further processing (Hackett et al., 2001; de la Mothe et al., 2006a,b; Padberg et al., 2009).

Alternate sections were stained for Nissl, PV immunohistochemistry (1:4,000 Sigma-Aldrich, St. Louis, MO), and NADPH-diaphorase histochemistry (Sherer-Singler et al., 1983). PV immunohistochemical reactions followed the protocol of the ABC method (ABC kit, Vector Laboratories, Burlingame, CA), and visualized with DAB or the Vector SG kit. Briefly, sections were blocked overnight in normal horse serum and incubated with the primary PV antibody (anti-PV in mouse, 1:4,000 Sigma-Aldrich) followed by a secondary mouse IgG (biotinylated antimouse IgG, 1:250; Vector Labs). NADPHd histochemistry uses the ability of this molecule to reduce the dye nitro blue tetrazoluim into an insoluble formazan (Fessenden and Schacht, 1998), which is visible with microscopy. Sections were incubated for 1 hour in a solution of 1 mg/ml nitroblue tetrazolium (Sigma Aldrich, N-6876), 0.5 mg/ml NADPH (Sigma-Aldrich, N-1630), and 0.1% Triton X-100 dissolved in 0.1 M phosphate buffer.

To determine the isotype specificity of the anti-PV antibody, the Sigma immunoType Kit (Product Code ISO-1) was used along with a double diffusion immunoassay using Mouse Monoclonal Antibody Isotyping Reagents (Product Code ISO-2). These procedures revealed isotype specificity as frog leg PV. Furthermore, in a study using monkey tissue immunoblotting of this antibody showed no crossreactivity, as suggested by a single band corresponding to 12 kD (Kultas-Ilinsky et al., 2011). Negative controls in which either the primary antibody (PV immunohistochemistry) or nitroblue tetrazolium (NADPHd histochemistry) were omitted revealed no positive signal, confirming that the secondary antibody and visualization reactions did not produce significant extraneous label. All antibodies, immunogen specificity, and chemicals used in these procedures are summarized in Table 2.

Data analysis

Standard light microscopy (Nikon D8000 microscope) techniques were used by two separate observers blind to the age of the animal to estimate the age-related changes in NADPHd+ and PV+ cell density of the CN. Counts were performed by digitally overlaying a 0.5 mm^2

grid on a 20× image of the CN. Sections where the grid could not be placed entirely within the boundaries of the CN were not counted to eliminate biases due to differences in counting area. The volume sampled by the counting grid was estimated by multiplying the known area of the grid (0.5 mm^2) by the tissue thickness (Table 1):

$$V_{ref}=0.5(T*n_{ref})$$

where T represents the tissue thickness and n_{ref} is the number of sections counted.

Differences in tissue thickness can result in overestimations of cell number due to the observer's inability to differentiate cell fragments at the planes in which the sections were cut (i.e., half cells look like whole cells), and thinner sections yield a greater proportion of fragmented cells. To avoid this bias an optical disector with a guard space of ¼ of a cell height was used (Mounton, 2002) so that estimated cell numbers (E_n) were calculated as:

$$E_n=N_v*V_{ref}$$

where

$$N_v=\sum Q/(n_{dis}*V_{dis})$$

where N_v represents the points counted in the volume, V_{ref} is the volume calculated by the Cavalieri principle, Q is the number of cells counted, n_{dis} is the number of disectors (sections counted), and V_{dis} is the volume of each disector. Since N_v and V_{ref} refer to a common volume, the total number of objects is estimated while controlling for volume changes (Mounton, 2002).

The density of the sample was defined as the cell count (E_n) divided by V_{ref}. Dorsal and ventral regions of each CN section were sampled and compared. These regions were located and sampled by randomly placing the counting grid at least twice within a single cochlear nucleus, once on the dorsal border and once on the ventral border of each region. In no animal was there a difference in positively stained cell density between the dorsal or ventral region of a section (paired *t*-test, $P > 0.1$), therefore densities were combined for analysis. Two independent observers blind to the identity of the animals sampled the CN. To ensure consistency the two observers counted the same noncochlear nucleus samples (SOC and IC) until they reached a 95% agreement or better for 20 consecutive samples. The CN was then sampled and counted independently by the two observers. A paired *t*-test showed that there was no difference in density calculations from the two observers (*t*-test; $P > 0.25$), and the densities were defined as the averages of the two observers counts.

Characterization of cochlear histopathologies

Detailed methods describing the histology and quantifications for the cochlear histopathologies used in this analysis can be found in Engle et al. (2012). Briefly, animals were anesthetized and euthanized using the same protocol described above. The temporal bone was chipped free, and the middle ear was exposed to puncture the round and oval

windows. The cochleae were decalcified using 0.35% EDTA until an acceptable level of decalcification was accomplished. The cochleae were cut semithinly (1 μm), mounted, and stained for toluidine blue and basic fuscin for brightfield microscopy. The densities of spiral ganglion cells and hair cells were calculated using standard light microscopy and unbiased stereological sampling techniques.

Statistical analysis

Statistical Analysis was done in two steps using SPSS v. 19 (Chicago, IL). First, the animals were categorized as middle-aged or old using 21.5 years (corresponding to ~65 human years) as the cutoff. There were four animals per group and their density values were compared using an unpaired *t*-test with a significance criterion of $P < 0.05$. Second, ABR-density relationships and cochlear histopathology-density relationships were analyzed by finding the Pearson product moment correlation along with a Monte Carlo analysis. This analysis was performed by randomly reassigning all values to new density values and finding the r-value of this random relationship. After 1,000 reassignments, the P-value was computed as the percentage of times that a random relationship gave an r-value greater than or equal to the observed r value. Therefore, the Monte Carlo provides the probability that the observed correlation is due to chance. To further ensure validity, these relationships were only considered significant if the $P < 0.05$ by the Monte Carlo (i.e., a regression coefficient was greater than 950/1,000 coefficients generated by chance), and if the r-squared value of the correlation exceeded 0.35.

RESULTS

The density of NADPHd and PV-positive neurons was determined in the CN of eight rhesus macaques (*Mac-acca mulatta*) ranging in age from 12 years and 3 months to 35 years and 7 months, roughly corresponding to 36 and 107 human years (see Table 1). We identified and characterized the CN into three principle subdivisions using the conventions of Ehret and Romand (1997) that are based on rostral-caudal and dorsal-ventral bifurcations of the auditory nerve. The rostral aspect of the rostral-caudal bifurcation creates the largest subdivision, the AVCN, and the posterior aspect of this bifurcation creates both the PVCN and DCN. A separate dorsal-ventral bifurcation differentiates the PVCN from the DCN. Figure 1 shows a PV-stained DCN (Fig. 1A), and an NADPHd-stained AVCN and PVCN (Fig. 1B,C, respectively). All three subnuclei stained positively for both stains in all animals, with the exception of a young animal (243 months), which inexplicably did not stain for NADPHd in any brain structure.

The first objective of this study was to characterize the NADPHd+ and PV+ cell densities in the different subdivisions of the CN as a function of natural aging. Visual inspection of this histological tissue subjectively revealed age-related changes in the density of NADPHd and PV, although to different extents in the three subdivisions. Qualitatively, the DCN and AVCN kept their expression of NADPHd relatively constant, while the PVCN appeared to increase its expression of these cell types, as shown in the high-magnification photomicrographs of the 15- and 35-year-old monkeys (Fig. 2). PV expression remained

more constant; however, a modest increase in density was observed in the DCN from these same animals (Fig. 3).

A major concern in any stereological analysis is the ability of an observer to differentiate positively labeled soma from the background neuropilar staining. A previous study from our laboratory using the same primate tissue demonstrated that observers can reliably make this distinction (Gray et al., 2013a). In that study, these same observers were able to reliably differentiate the positively stained cells in the lateral and medial superior olives, which had much higher background staining than what is seen in any of the subdivisions in the CN (compare Figs. 2 and 3 with Gray et al., 2013a, figs. 2 and 3). We are therefore confident that the observers reliably differentiated positively labeled neurons from background staining in this analysis.

We next quantified these qualitative impressions by sampling positively labeled cells within the AVCN, PVCN, and DCN of each animal and calculating the densities of reactive neurons to both markers (see Materials and Methods). Comparisons were made between animals that were classified as middle-aged (12.3–20.4 years; roughly 37 to 61 human years) or old (22.3–35.6; roughly 66 to 107 human years). The results showed that NADPHd+ cell density was not statistically different between age groups in either the AVCN or DCN (unpaired *t*-test; $P > 0.05$; Fig. 4A), but significantly increased in the aged PVCN (unpaired *t*-test $P < 0.05$; Fig. 4A). In contrast, the densities of PV-positive neurons did not change in any subdivision of the CN with age (all $P > 0.05$; Fig. 4B).

The classification of monkeys into middle age vs. aged allows one to perform relatively simple statistical analysis, although it is somewhat arbitrary. Additionally, many previous studies have shown a great deal of individual variability across a broad range of metrics of age-related hearing loss (reviewed by Davis et al., 2003). To determine whether the differences as a function of age, or the lack thereof, could be due to this normal variability, we performed regression analysis to further test for age-related effects. Figure 4C shows the changes of NADPHd cell density in the PVCN as a function of age ($r = 0.89$, $P < 0.01$). The high correlation coefficient of this statistically significant relationship suggests that the age-related increases in NADPHd+ neurons are not due to natural variability, but rather systematic increases. Regression analyses between age and NADPHd densities of the AVCN and DCN revealed insignificant relationships with lower correlation coefficients (*r* values 0.60 and 0.54 in the AVCN and DCN, respectively; all $P > 0.05$), and similarly, PV density and age did not significantly correlate in any subdivision (*r* values of 0.40, 0.53, and 0.81 in PVCN, AVCN, and DCN, respectively; all $P > 0.05$), although the DCN showed a strong increasing trend.

Changes seen were specific to the CN

The preceding analysis shows that cells in the CN increased their expression of NADPHd in the PVCN as a function of age. This raises the question of whether the neurochemical changes noticed were a result of aging processes specific to the CN, or simply the effects of aging on neural tissue at this level of the brainstem. Previous age-related neurochemical studies in the macaque SOC show more pronounced age-related increases of these two neurochemical markers within specific auditory structures compared to the surrounding

tissue (Gray et al., 2013a). It is also the case that some subdivisions do not show the same degree of age-related effects as others (e.g., the PVCN compared to the AVCN). These results indicate that the changes in the CN are not a result of general changes in the nervous system, vascularization, fixation of the tissue, or other nonspecific histological processes, but rather inherent to the aging CN.

Changes in ABR peak II amplitudes correlate with PV density

A previous study in the macaque SOC demonstrated a relationship between cell density and ABR peak IV amplitudes (the peak to which the SOC is thought to contribute most to). To investigate the relationship between NADPHd and PV density changes with the ABR, we performed regression analysis between these densities and peak II, as the CN contributes predominantly to this peak (Møller and Burgess, 1986). ABR wave II amplitudes and latencies were quantified in seven of these animals (see Table 1). The stimuli used in this analysis consisted of clicks, low, middle, and high-frequency tones presented at 70 dB SPL and ABR threshold (see Materials and Methods). The 70 dB stimulus was suprathreshold for all animals except for the oldest with some stimuli. At the first level of analysis we correlated the NADPHd1 and PV1 cell densities from each subdivision with wave II amplitudes and latencies, and found no significant relationships. Given that all three subnuclei presumably contribute to the formation of wave II, we also combined the density values of the three subdivisions and correlated these values with wave II amplitudes and latencies. This analysis revealed that the peak II latencies for any stimulus were not correlated with cell density, which is consistent with what was reported previously for the SOC (Gray et al., 2013a). Similarly, peak II amplitudes evoked by low and middle frequency (0.5–8 kHz) stimuli at any intensity also did not correlate with the densities of either cell type (all $P > 0.3$). In contrast, the PV1 cells were significantly correlated with high-frequency (12–16 kHz) ABR amplitudes at both 70 dB SPL ($r = -0.774$, $P < 0.05$; Fig. 5A, black lines and points) and at ABR threshold ($r = 20.703$; $P < 0.05$; 5C), and trended with click amplitudes at threshold ($r = 20.646$, $P = 0.09$; Fig. 5D). The inverse correlation indicates that PV densities decreased as ABR amplitudes increased. NADPHd+ cells had little tendency to correlate with any ABR property, and only showed statistical significance by our criteria with 70 dB click amplitudes ($r = -0.899$, $P < 0.05$; Fig. 5B; gray points and lines). These results suggest that at the level of the CN, PV+ cells relate more to changing properties of the ABR than do NADPHd+ cells, and these relationships are seen with high-frequency processing.

Cochlear histopathologies correlate with cell densities

The basal turn of the cochlea is the primary high-frequency transduction region, and shows the greatest age-related declines in hair cell and spiral ganglion cell density. Since these histopathologies occur in cells that synapse on cells of the CN or are only one synapse upstream, we analyzed the relationship of these histopathologies with the age-related density changes of the CN described above. With this analysis we hoped to reveal which protein, PV or NADPHd, relates most to these changes, and compare those results to PV and NADPHd relationships with the ABRs described above (Fig. 5).

Five monkeys from the current study had been previously used to quantify age-related cochlear histopathologies (Engle et al., 2012), which demonstrated the loss of inner hair cells (IHC), outer hair cells (OHC), and spiral ganglion cells (SGC). One of these animals was the young monkey that showed no staining for NADPHd in any neural structures (see Materials and Methods), so the sample size was further restricted to four monkeys. Several interesting results were noted in this analysis despite the small sample size. First, PV+ neuron density in the AVCN and DCN were the only cell densities to show significant relationships with OHC loss ($r = -0.93$, $P < 0.05$; $r = -0.89$, $P < 0.05$ for AVCN and DCN, respectively; Fig. 6A). Second, while similar analysis with the density of NADPHd+ neurons did not reach statistical significance, there were good correlation coefficients ($r = 0.90$; $P = 0.19$; 0.94, $P = 0.15$ for AVCN and DCN, respectively; Fig. 6B). This is likely due to the small sample size (see above). Third, there were no statistically significant correlations, or trends for either stain in any of the three CN subdivisions tested for inner hair cell loss or spiral ganglion cell loss (all $P > 0.05$). Together, these results imply that PV density, and perhaps NADPHd density, relates only to OHC loss, which suggests an interaction between the two processes.

DISCUSSION

The present study attempts to further elucidate the age-related chemical changes of the macaque ascending auditory system. Although these studies are relatively sparse in the macaque, both the SOC (Gray et al., 2013a) and IC (unpubl. obs.) show increases in NADPHd+ and PV+ cell densities with increasing age. In these two auditory nuclei the age-related density changes were only seen in specific subdivisions, for example, only in the medial superior olive but not the lateral superior olive or medial nucleus of the trapezoid body (Gray et al., 2013a). Our current results are consistent in that the cell density in the PVCN was the only subdivision with a statistically significant increase, and only for NADPHd, not PV. Thus, like the IC and SOC, age does not affect the anatomically and functionally defined regions of the CN equivalently. These results, combined with those of the other two macaque studies, provide strong evidence against these results being the product of nonspecific effects of natural aging on the tissue. Rather, it seems that a specific auditory subpathway expresses these changes, and why this is the case remains unclear.

Anatomical changes in the ascending auditory system has previously been demonstrated in the SOC (Gray et al., 2013a), and now in the major input to the SOC, the CN. These CN results suggest that these chemical changes do occur at the lowest level of the central auditory system, although not for all chemical markers. Unlike in higher auditory structures, PV+ cell densities remained constant with age in the CN. Whether other calcium-binding proteins change their expressions in the macaque CN remains to be seen. NADPHd colocalizes with several calcium-binding proteins throughout the brain (Yan et al., 1996; Soares-Mota et al., 2001), therefore the age-related increase in the PVCN suggests that non-PV calcium-binding proteins may increase as well. This would be consistent with the calbindin and calretinin increases seen in the aged cochlear nucleus of mice, although increases in PV are also seen in this animal model (Idrizbegovic, 2003, 2004, 2006).

The age-related changes that we noted were confined to the PVCN. This observation is also consistent with the rodent CN, where only specific subdivisions change with age (Idrizbegovic, 2003, 2004, 2006). Furthermore, in other auditory nuclei, only specific subdivision show these changes as well (Zettel et al., 1997; Reuss et al., 2000; Ouda et al., 2003, 2008; Sanchez-Zuriaga et al., 2007; Huh et al., 2008; Gray et al., 2013a). Therefore, the PVCN seems to be part the auditory subpathway (discussed above) that experiences neurochemical changes with age. Again, why only specific subdivisions change as a function of age is an open question. The auditory system is comprised of parallel processing streams that are chemically defined, and somewhat independent from each other (Jones, 2003). Therefore, it is likely that these age-related effects are found within one of these streams, but not the others. In the CN, this hypothesis is difficult to understand since these processing streams overlap extensively here compared to higher auditory structures where they become more segregated.

Previous studies in rodents have shown a great variability in the direction and magnitude of similar chemical changes between species, strain, and auditory structure (Zettel et al., 1997; Reuss et al., 2000; Ouda et al., 2003, 2008; Sanchez-Zuriaga et al., 2007; Huh et al., 2008). In contrast to both increases and decreases of these chemical markers with age in rodents, our macaque data have only shown density increases, when changes do occur (current study; Gray et al., 2013a). These differences between animal models suggest that different age-related changes can occur, and should not be generalized across species; although it must be kept in mind that all reports in the macaque are from the same set of histological tissue and thus the variability is unknown.

These studies did not attempt to define changes in morphological classes of neurons, but rather their immunoreactivities to PV and NADPHd. Although in the CN morphological classes of neurons are well defined (reviewed by Oertel et al., 2011), these analyses are rarer in higher auditory structures. Also, it is unclear whether all neurons within a morphological class express PV or NADPHd. Therefore, studies investigating age-related neurochemical changes generally do not attempt to define morphological cell classes in their analysis. To be consistent with previous reports and to avoid introducing further variables, the present study did not attempt to define morphology. It is possible, however, that specific cell types expressing either NADPHd or PV are responsible for the changes seen with age.

NO and PV functions in the brainstem

It has become increasingly clear that with increased age and hearing thresholds NADPHd+ and PV+ cells change their expressions within the ascending auditory pathway of mammals. The role of these cell types in audition, however, remains unclear. While there is a general consensus that these cell types play important roles in the auditory system, the precise mechanisms by which these cells work, and even whether they are physiologically excitatory or inhibitory at different nuclei, remains speculative.

NO is the product of NADPHd's action, and has been associated with numerous activities throughout the nervous system (Esplugues, 2002), yet its primary role is likely as a signaling molecule used for both neuro-transmission and neuromodulation. The consistent age-related changes in expression of NADPHd suggests that NO may also play a compensatory role in

the aging process. Previous chemical and physiological studies have shown that the excitability of neurons in the auditory system increases with age (Caspary et al., 2005, 2006; Juarez-Salinas et al., 2010; Engle and Recanzone, 2012) in spite of a decrease in hair cells and spiral ganglion cells in the cochlea (e.g., see Engle et al., 2012). NO has been shown to depress glut-NMDA receptors, suggesting it may play a role in preventing glutamate excitotoxicity (Manzoni and Bockaert, 1993). In the case of natural aging, it may act to compensate for the increased excitability of central auditory neurons. Our finding that the density of NADPHd+ neurons and cochlear histopathologies were not correlated support this view because it indicates that NADPHd does not relate to peripheral hearing loss. However, given the small sample size this interpretation merits caution.

PV's role in the brainstem is also unclear. In the neo-cortex, PV+ interneurons are a major class of GABAergic inhibitory neurons (Rudy and Fishell, 2010), where their role is thought to be well understood. However, colocalization studies of PV with markers for GABA, glutamate, and glycine neurotransmission in the CN, SOC, and IC of rodents and nonhuman primates show very different results. PV-positive cells in the CN and SOC primarily colocalize with glutamate, whereas in the IC these cells primarily colocalize with GABA (Fredrich et al., 2009; Gray et al., 2013b). Additionally, this coloc-alization is not complete, as is seen in the cerebral cortex, so PV+ cells in these structures could have a fundamentally different physiological role and/or comprise a number of different types of neurons. Nonetheless, one plausible reason that PV increases in brainstem auditory areas could also be due to the increased excitability of these neurons with increasing age. As PV acts as a calcium buffer, it may act to reduce the toxic effects of calcium influx in neurons with high activity, similar to the role of NADPHd noted above. In the CN and SOC, the significant correlations seen between PV+ neuron densities and various physiological tests support this hypothesis (current study; Gray et al., 2013a). As with NADPHd+ neurons, further studies describing PV+ cells in the brainstem are necessary to understand PV's subcortical role, and consequently the impact of the age-related changes in the expression of these proteins.

PV density correlates with ABR peak II amplitude and cochlear histopathologies

In the CN, PV+ cell densities increased as the ABR peak II amplitudes decreased. Similar inverse relationships were noted between cell densities of the SOC and peak IV amplitudes (Gray et al., 2013a). The ABR is a broad-spectrum signal arising from the summation of synaptic potentials, so this correlation is counterintuitive, as PV+ cells seem to be excitatory in the brainstem (Fredrich et al., 2009; unpubl. obs.), and increased densities should result in increased peak II amplitudes. However, ABR amplitudes largely reflect the temporal precision of the neural signal, not the absolute number of action potentials. This indicates that increases in PV could be associated with age-related decreases in the temporal precision of activity as early as the cochlear nucleus.

The correlations between density and peak II amplitude were only present when high-frequency and click stimuli were used, but not with low- or middle-frequency stimuli. Similar results were shown in the SOC of the macaque, where NADPHd and PV densities correlated only when high-frequency and click stimuli were used. ABR thresholds to low- and middle-frequency tones are not strongly affected by age (Navarro et al., 2008),

indicating that the neural responses to lower-frequency stimuli are either unaffected by the aging process, or that compensatory mechanisms ensure their constancy with age. The latter view suggests that PV+ cells may be involved in the maintenance of neural responses, and fails to achieve this constancy in the response to high-frequency tones.

Alternatively, the correlations seen with high-frequency tones may simply reflect less high-frequency processing in the CN due to less transduction of these frequencies at the inner ear. In the macaque, the basal turn of the cochlea, which corresponds to the high-frequency transduction region, loses SGCs, IHCs, and OHCs to the greatest extent with age (Engle et al., 2012). The cochlear nucleus is thought to be tonotopically organized, thus one could expect age-related changes to be most prominent at certain frequency representation as seen in the cochlea. Although this question was not tested systematically, counting grids were placed at various locations of each subdivision, and statistical analysis suggests that there were no differences in the age-related changes as a function of the frequency representation of the area. This agrees with Gray et al. (2013a), where age-related neurochemical changes were systematically studied as a function of tonotopy in the SOC. This study reports age-related changes in the medial superior olive that are independent the frequency representation of the neurons. Therefore, frequency specific neurochemical changes do not seem to be present in the auditory brainstem.

An interesting result of this study is that PV related significantly with ABRs as discussed above and with cochlear histopathologies, but not with age. NADPHd, however, only showed a significant relationship with age, but not with the ABR or cochlear histopathologies. This dissociation begins to suggest that if PV and NADPHd do in fact play compensatory roles in the aging auditory system, they likely take part in distinct efforts.

Although SGC, IHC, and OHC all decrease in number with age, only the decrease in OHC number was significantly correlated with PV density within the AVCN and DCN. Outer hair cells do not transduce sounds directly, but rather are the recipients of descending projections that drive these cells to function as cochlear amplifiers, presumably improving the quality of the sound signal (Mellado Lagarde et al., 2008). The IHCs and SGCs, however, both transduce sound and deliver this neural signal to the CN, and are thus both considered the beginning of an ascending pathway. Therefore, PV changes in the CN may be part of a descending pathway affected by the aging process. In this view, PV’s relationship to the changing ABR reflects physiological differences due to changes in amplification at the cochlea rather than sound transduction. NADPHd may not to be associated with this potential pathway since its density does not significantly correlate with any cochlear histopathology, and also because its age-related changes in expression were found in a different subdivision (PVCN) than where the PV-OHC relationships were noted (AVCN and DCN). Whether NADPHd is or is not a part of this descending pathway is difficult to determine with this small sample size; however, statistically it does not. Regardless, the AVCN and DCN correlate only with OHC densities and not age, unlike the PVCN, which only correlates with age. These results suggest that these three subdivisions correspond to different age-related processes, and their neurochemical changes may reflect this dissociation with NADPHd.

In these views, age-related PV changes relate to and may be a part of changing descending auditory projections, while NADPHd may not be associated with either ascending or descending pathways, but possibly directly to a subset of aged neurons. As discussed above, NO potentially plays a role in combating excitotoxicity, and being that the auditory system is an active system whose excitability increases with age (Caspary 1995, 1998, 2008), this likely is a problem the aged auditory system must face. Most important, however, these observations suggest that aging and age-related hearing deficits are separable processes, and the roles of PV and NADPHd may be distinguishable in this regard.

Acknowledgments

The authors thank Xochi Navarro, Dina Juarez-Salinas, Anastasiya Petrovska, and Marianthi Gelatos for help with this project, and Rhonda Oates-O'Brien and Guy Martin for excellent animal care.

Grant sponsor: National Institute on Aging (NIA); Grant numbers: R21AG024372; R01AG034137 (to G.H.R.); Grant sponsor: National Institute on Deafness and Other Communication Disorders (NIDCD); Grant number: T32DC008072 (to J.R.E.).

LITERATURE CITED

Allen AR, Starr A. Auditory brain stem potentials in monkey (M. mulatta) and man. Electroencephalogr Clin Neurophysiol. 1978; 45:53–63. [PubMed: 78822]

Bennet CL, Davis RT, Miller JM. Demonstration of presbycusis across repeated measures in a nonhuman primate species. Behav Neurosci. 1983; 97:602–607. [PubMed: 6615636]

Bredt DS, Snyder SH. Isolation of nitric oxide synthetase, a calmodulin-requiring enzyme. Proc Natl Acad Sci U S A. 1990; 87:682–685. [PubMed: 1689048]

Brenman JE, Chao DS, Gee SH, McGee AW, Craven SE, Santillano DR, Wu Z, Huang F, Xia H, Peters MF, Froehner SC, Bredt DS. Interaction of nitric oxide syn-thase with the postsynaptic density protein PSD-95 and alpha1-syntrophin mediated by PDZ domains. Cell. 1996; 84:757–767. [PubMed: 8625413]

Caspary DM, Milbrandt JC, Helfert RH. Central auditory aging: GABA changes in the inferior colliculus. Exp Gerontol. 1995; 30:349–360. [PubMed: 7556513]

Caspary DM, Holder TM, Hughes LF, Milbrandt JC, McKernan RM, Naritoku DK. Age-related changes in GABA(A) receptor subunit composition and function in rat auditory system. Neuroscience. 1999; 93:307–312. [PubMed: 10430494]

Caspary DM, Schatteman TA, Hughes LF. Age-related changes in the inhibitory response properties of dorsal cochlear nucleus output neurons: role of inhibitory inputs. J Neurosci. 2005; 25:10952–10959. [PubMed: 16306408]

Caspary DM, Hughes LF, Schatteman TA, Turner JG. Age-related changes in the response properties of cartwheel cells in rat dorsal cochlear nucleus. Hear Res. 2006; 216–217:207–215.

Caspary DM, Ling L, Turner JG, Hughes LF. Inhibitory neurotransmission, plasticity and aging in the mammalian central auditory system. J Exp Biol. 2008; 211:1781–1791. [PubMed: 18490394]

Davis, RT.; Leathers, CW. Behavior and pathology of aging in rhesus monkeys. New York: A.R Liss; 1985.

Davis RR, Kozel P, Erway LC. Genetic influences in individual susceptibility to noise: a review. Noise Health. 2003; 5:19–28. [PubMed: 14558889]

de la Mothe LA, Blumell S, Kajikawa Y, Hackett TA. Cortical connections of the auditory cortex in marmoset monkeys: core and medial belt regions. J Comp Neurol. 2006a; 496:27–71. [PubMed: 16528722]

de la Mothe LA, Blumell S, Kajikawa Y, Hackett TA. Thalamic connections of the auditory cortex in marmoset monkeys: core and medial belt regions. J Comp Neurol. 2006b; 496:72–96. [PubMed: 16528728]

Disterhoft JF, Moyer JR Jr. Thomson LT. The calcium rationale in aging and Alzheimer's disease. Evidence from an animal model of normal aging. Ann N Y Acad Sci. 1995; 747:382–406. [PubMed: 7847686]

Ehret, G.; Romand, R. The central auditory system. New York: Oxford University Press; 1997.

Engle JR, Recanzone GH. Characterizing spatial tuning functions of neurons in the auditory cortex of young and aged monkeys: a new perspective on old data. Frontiers Aging Res. 2012; 4:36.

Engle JR, Tinling S, Recanzone GH. Age-related hearing loss in rhesus monkeys is correlated with cochlear histopathologies. PLoS ONE. 2013; 8:e55092. [PubMed: 23390514]

Esplugues JV. NO as a signalling molecule in the nervous system. Br J Pharmacol. 2002; 135:1079–1095. [PubMed: 11877313]

Fessenden JD, Schacht J. The nitric oxide/cyclic GMP pathway: a potential major regulator of cochlear physiology. Hear Res. 1998; 118:168–176. [PubMed: 9606072]

Fetoni AR, Picciotti PM, Paludetti G, Troiani D. Pathoge-nesis of presbycusis in animal models: a review. Exp Gerentol. 2011; 46:413–425.

Fowler CG, Chiasson KB, Leslie TH, Thomas D, Beasley TM, Kemnitz JW, Weindruch R. Auditory function in rhesus monkeys: effects of aging and caloric restriction in the Wisconsin monkeys five years later. Hear Res. 2010; 261:75–81. [PubMed: 20079820]

Fredrich M, Reisch A, Benjamin-Illing R. Neuronal subtype identity in the rat auditory brainstem as defined by molecular profile and axonal projection. Exp Brain Res. 2009; 195:241–260. [PubMed: 19340418]

Gray DT, Engle JR, Recanzone GH. Age-related neurochemical changes in the rhesus macaque superior olivary complex. J Comp Neurol. 2013a [Epub ahead of print].

Gray DT, Engle JR, Rudolph ML, Recanzone GH. Molecular profiles of parvalbumin and calbindin positive neurons in the rhesus macaque auditory midbrain and brainstem. Soc Neurosci Abstr. 2013b

Hackett TA, Preuss TM, Kaas JH. Architectonic identification of the core region in auditory cortex of macaques, chimpanzees, and humans. J Comp Neurol. 2001; 441:197–222. [PubMed: 11745645]

Hawkins, JE.; Miller, JM.; Rouse, RC.; Davis, JA.; Rarey, K. Inner ear histopathology in aging rhesus monkeys (*Macaca mulatta*). In: Davis, RT.; Leathers, CW., editors. Behavior and pathology of aging in rhesus monkeys. New York: Liss; 1986.

Hopper R, Lancaster B, Garthwaite J. On the regulation of NMDA receptors by nitric oxide. Eur J Neurosci. 2004; 19:1675–1682. [PubMed: 15078541]

Huh Y, Choon Park D, Geun Yeo S, Cha Il C. Evidence for increased NADPH-diaphorase-positive neurons in the central auditory system of the aged rat. Acta Otolaryngol. 2008; 128:648–653. [PubMed: 18568499]

Idrizbegovic E, Bogdanovic N, Viberg A, Canlon B. Auditory peripheral influences on calcium binding protein immunoreactivity in the cochlear nucleus during aging in the C57BL/6J mouse. Hear Res. 2003; 179:33–42. [PubMed: 12742236]

Idrizbegovic E, Bogdanovic N, Willott JF, Canlon B. Age-related increases in calcium-binding protein immunoreactivity in the cochlear nucleus of hearing impaired C57BL/6J mice. Neurobiol Aging. 2004; 25:1085–1093. [PubMed: 15212833]

Idrizbegovic E, Salman H, Niu X, Canlon B. Presbyacu-sis and calcium-binding protein immunoreactivity in the cochlear nucleus of BALB/c mice. Hear Res. 2006; 216–217:198–206.

Jones EG. Chemically defined parallel pathways in the monkey auditory system. Ann N Y Acad Sci. 2013; 999:218–233. [PubMed: 14681146]

Juarez-Salinas DL, Engle JR, Navarro XO, Recanzone GH. Hierarchical and serial processing in the spatial auditory cortical pathway is degraded by natural aging. J Neurosci. 2010; 30:14795–14804. [PubMed: 21048138]

Laughlin NK, Hartup BK, Lasky RE, Meier MM, Hecox KE. The development of auditory event related potentials in the rhesus monkey (Macaca mulatta). Dev Psychobiol. 1999; 34:37–56. [PubMed: 9919432]

Loftus WC, Malmierca MS, Bishop DC, Oliver DL. The cytoarchitecture of the inferior colliculus revisited: a common organization of the lateral cortex in rat and cat. Neuroscience. 2008; 154:196–205. [PubMed: 18313229]

Kultas-Ilinsky K, Ilinsky IA, Verney C. Glutamic acid decarboxylase isoform 65 immunoreactivity in the motor thalamus of humans and monkeys: c-aminobutyric acid-ergic connections and nuclear delineations. J Comp Neurol. 2011; 519:2811–2837. [PubMed: 21491431]

Manzoni O, Bockaert J. Nitric oxide synthase activity endogenously modulates NMDA receptors. J Neurochem. 1993; 61:368–370. [PubMed: 7685816]

Mellado Lagarde MM, Drexl M, Lukashkina VA, Lukashkin AN, Russell IJ. Outer hair cell somatic, not hair bundle, motility is the basis of the cochlear amplifier. Nat Neurosci. 2008; 11:746–748. [PubMed: 18516034]

Møller AR, Burgess J. Neural generators of the brainstem auditory evoked potentials (BAEPs) in the rhesus monkey. Electroencephalogr Clin Neurophysiol. 1986; 65:361–372. [PubMed: 2427327]

Mounton, PR. Principles and practices of unbiased stereology. Baltimore: Johns Hopkins University Press; 2002.

Navarro X, Engle J, Fletcher M, Juarez-Salinas D, Recanzone GH. Age-related changes in the auditory brainstem response to tones and noise in macaque monkeys. Soc Neurosci Abstr. 2008; 34

Oertel D, Wright S, Cao XJ, Ferragamo M, Bal R. The multiple functions of T stellate/multipolar/chopper cells in the ventral cochlear nucleus. Hear Res. 2011; 276:61–69. [PubMed: 21056098]

Ouda L, Nwabueze-Ogbo FC, Druga R, Syka J. NADPH-diaphorase-positive neurons in The auditory cortex of young and old rats. Neuroreport. 2003; 14:363–366. [PubMed: 12634484]

Ouda L, Druga R, Syka J. Changes in parvalbumin immunoreactivity with aging in the central auditory system of the rat. Exp Gerontol. 2008; 43:782–789. [PubMed: 18486384]

Padberg J, Cerkevich C, Engle J, Rajan AT, Recanzone G, Kaas J, Krubitzer L. Thalamocortical connections of parietal somatosensory cortical fields in macaque monkeys are highly divergent and convergent. Cerebral Cortex. 2009; 19:2038–2064. [PubMed: 19221145]

Reuss S, Schaeffer DF, Laages MH, Riemann R. Evidence for increased nitric oxide production in the auditory brain stem of the aged dwarf hamster (Phodopus sungorus): an NADPH-diaphorase histochemical study. Mech Ageing Dev. 2000; 112:125–134. [PubMed: 10690925]

Rudy B, Fishell G, Lee S, Hjerling-Leffler J. Three groups of interneurons account for nearly 100% of neocortical GABAergic neurons. Dev Neurobiol. 2011; 71:45–61. [PubMed: 21154909]

Sanchez-Zuriaga D, Marti-Gutierrez N, De La Cruz MA, Peris-Sanchis MR. Age-related changes of NADPH-diaphorase-positive neurons in the rat inferior colliculus and auditory cortex. Microsc Res Tech. 2007; 70:1051–1059. [PubMed: 17722059]

Scherer-Singler U, Vincent SR, Kimura H, McGeer EG. Demonstration of a unique population of neurons with NADPH-diaphorase histochemistry. J Neurosci Methods. 1983; 9:229–234. [PubMed: 6363828]

Soares-Mota M, Henze I, Mendez-Otero R. Nitric oxide synthase-positive neurons in the rat superior colliculus: colocalization of NOS with NMDAR1 glutamate receptor, GABA, and parvalbumin. J Neurosci Res. 2001; 64:501–507. [PubMed: 11391705]

Tang AH, Karson MA, Nagode DA, McIntosh JM, Uebele VN, Renger JJ, Klugmann M, Milner TA, Alger BE. Nerve terminal nicotinic acetylcholine receptors initiate quantal GABA release from perisomatic interneurons by activating axonal T-type (Cav3) Ca2_ channels and Ca2_release from stores. J Neurosci. 2011; 31:13546–13561. [PubMed: 21940446]

Toescu EC, Vreugdenhil M. Calcium and normal ageing. Cell Calcium. 2010; 42:158–164. [PubMed: 20045187]

Torre, P3rd; Fowler, CG. Age-related changes in auditory function of rhesus monkeys (Macaca mulatta). Hear Res. 2000; 142:131–140. [PubMed: 10748335]

Torre, P3rd; Mattison, JA.; Fowler, CG.; Lane, MA.; Roth, GS.; Ingram, DK. Assessment of auditory function in rhesus monkeys (Macaca mulatta): effects of age and calorie restriction. Neurobiol Aging. 2004; 25:945–954. [PubMed: 15212848]

Yan XX, Jen LS, Garey LJ. NADPH-diaphorase-positive neurons in the primary cerebral Cortex colocalize withGABA and calcium binding proteins. Cerebral Cortex. 1996; 6:524–529. [PubMed: 8670678]

Zettel ML, Frisina RD, Haider SE, O'Neill WE. Age-related changes in calbindin D-28k and calretinin immunoreactivity in the inferior colliculus of CBA/CaJ and C57Bl/6 mice. J Comp Neurol. 1997; 386:92–110. [PubMed: 9303527]

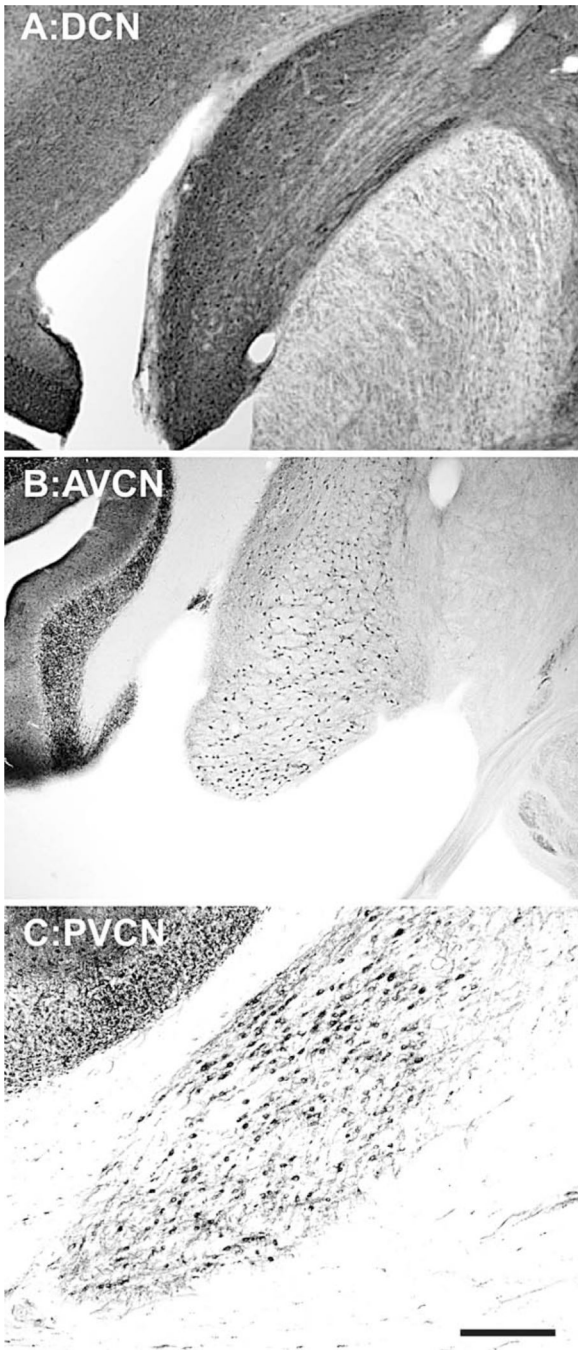

Figure 1.

Anatomical subdivisions of the macaque cochlear nucleus. Transverse parvalbumin stained sections through the **(A)** dorsal cochlear nucleus (DCN), and transverse NADPH-diaphorase stained sections through the **(B)** the anterior ventral cochlear nucleus (AVCN), and the **(C)** posterior ventral cochlear nucleus (PVCN). The right side of each image corresponds to the medial aspect, and the top to the dorsal aspect of the section. Scale bar = 500 μm.

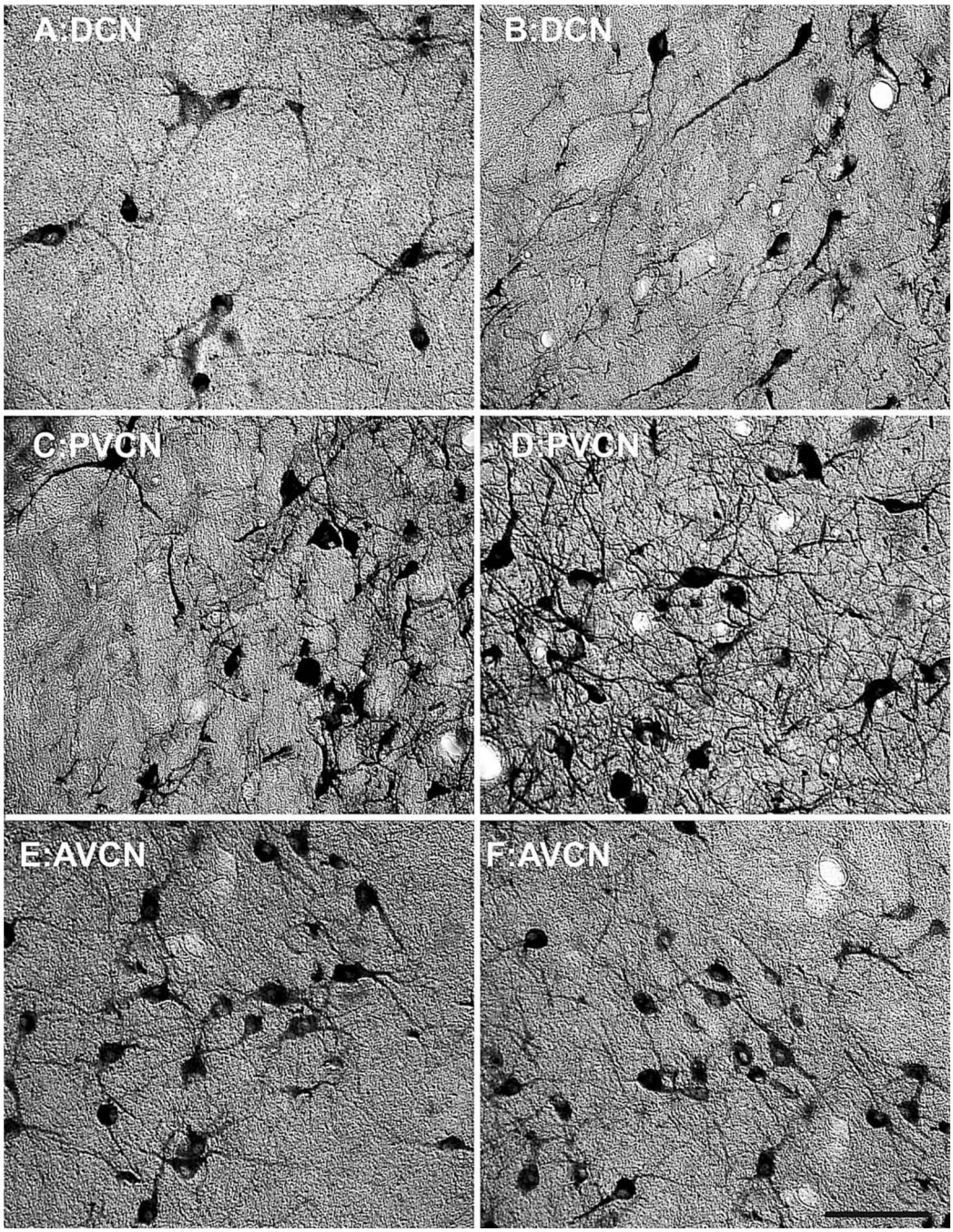

Figure 2.

Comparison of NADPH-diaphorase (NADPHd) cell density of the cochlear nucleus between a 15- and 35-year-old animal. Comparison of micrographs from a **(A)** 15-year-old dorsal cochlear nucleus (DCN) and **(B)** 35-year-old DCN reveals no apparent age related changes in density. Similarly, when comparing a **(C)** 15-year-old anterior ventral cochlear nucleus (AVCN) with a **(D)** 35-year-old AVCN, no age-related density changes become apparent. However, posterior ventral cochlear nucleus (PVCN) showed clear age-related increases in

NADPHd between the **(E)** 15-year-old and **(F)** 35-year-old animals. Dorsal is up and medial toward the left. Scale bar = 150 μm.

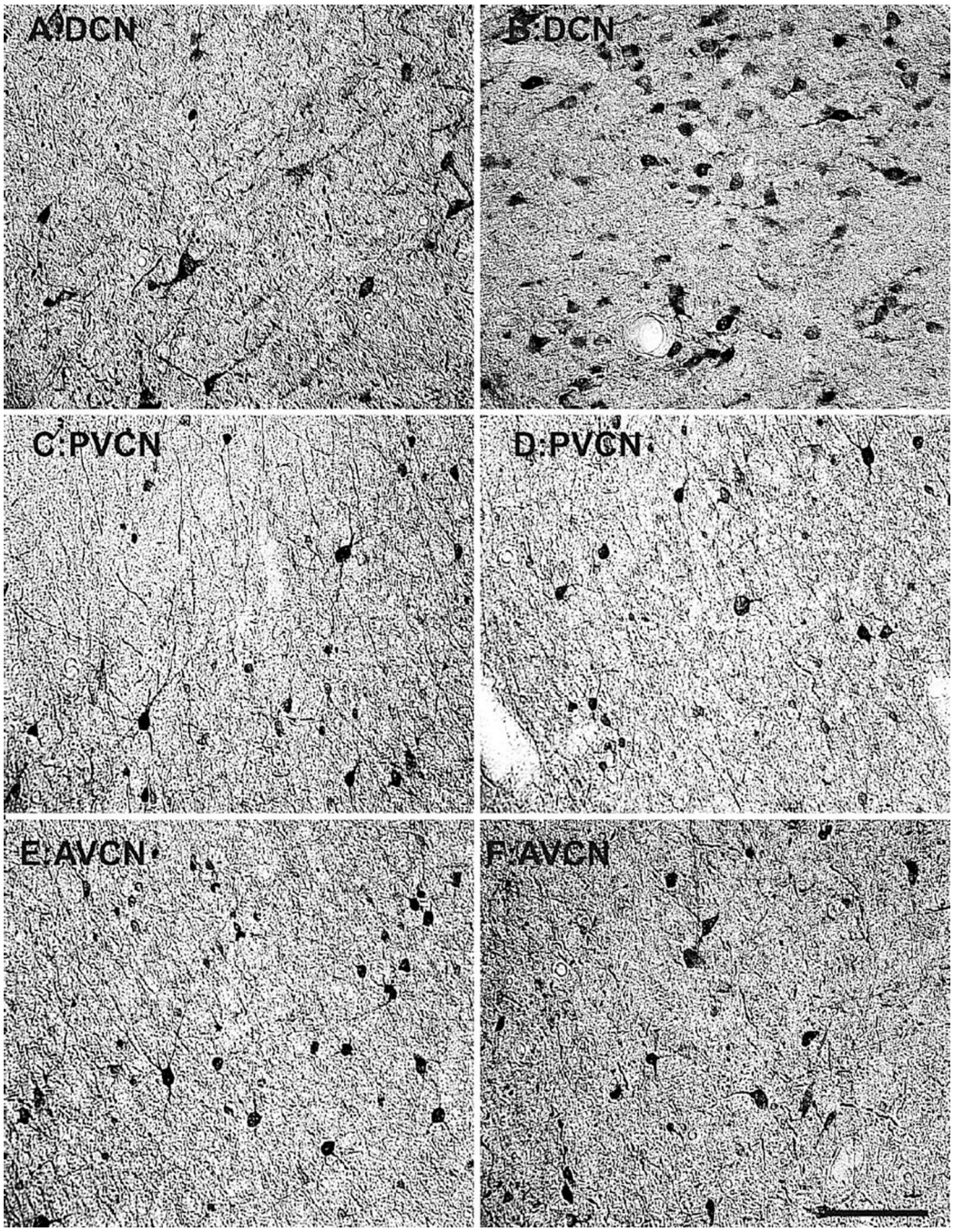

Figure 3.

Comparison of parvalbumin (PV)-positive cell density of the SOC between a 15- and 35-year-old animal. Comparison of micrographs from a **(A)** 15-year-old dorsal cochlear nucleus (DCN) and **(B)** 35-year-old DCN reveals modest age-related changes in PV density. However, when comparing a (C) 15-year-old anterior ventral cochlear nucleus (AVCN) with a (D) 35-year-old AVCN, no age-related density changes become apparent. Similarly, the posterior ventral cochlear nucleus (PVCN) of the **(E)** 15-year-old or **(F)** 35-year-old animals did not differ. Conventions as in Fig. 2. Scale bar = 200 μm.

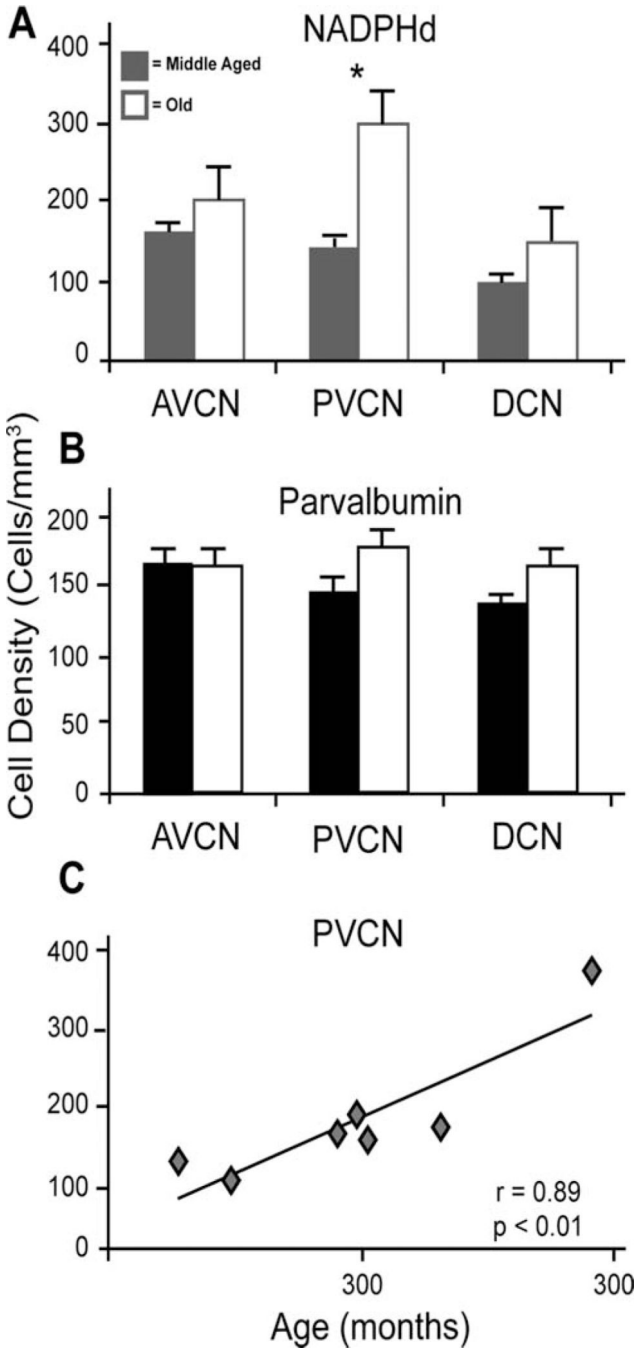

Figure 4.

Estimated cell densities from the three subdivisions of the cochlear nucleus. An age-related comparison of **(A)** NADPH-diaphorase (NADPHd)-positive and **(B)** parvalbumin (PV)-positive cell densities in the dorsal cochlear nucleus (DCN), anterior ventral cochlear nucleus (AVCN), and posterior ventral cochlear nucleus (PVCN). Solid bars represent middle-aged density averages, and white bars represent density averages from aged animals. Significant increases of NADPHd were noted only within the PVCN. **C**: NADPHd+ cell densities of the PVCN as a function of age.

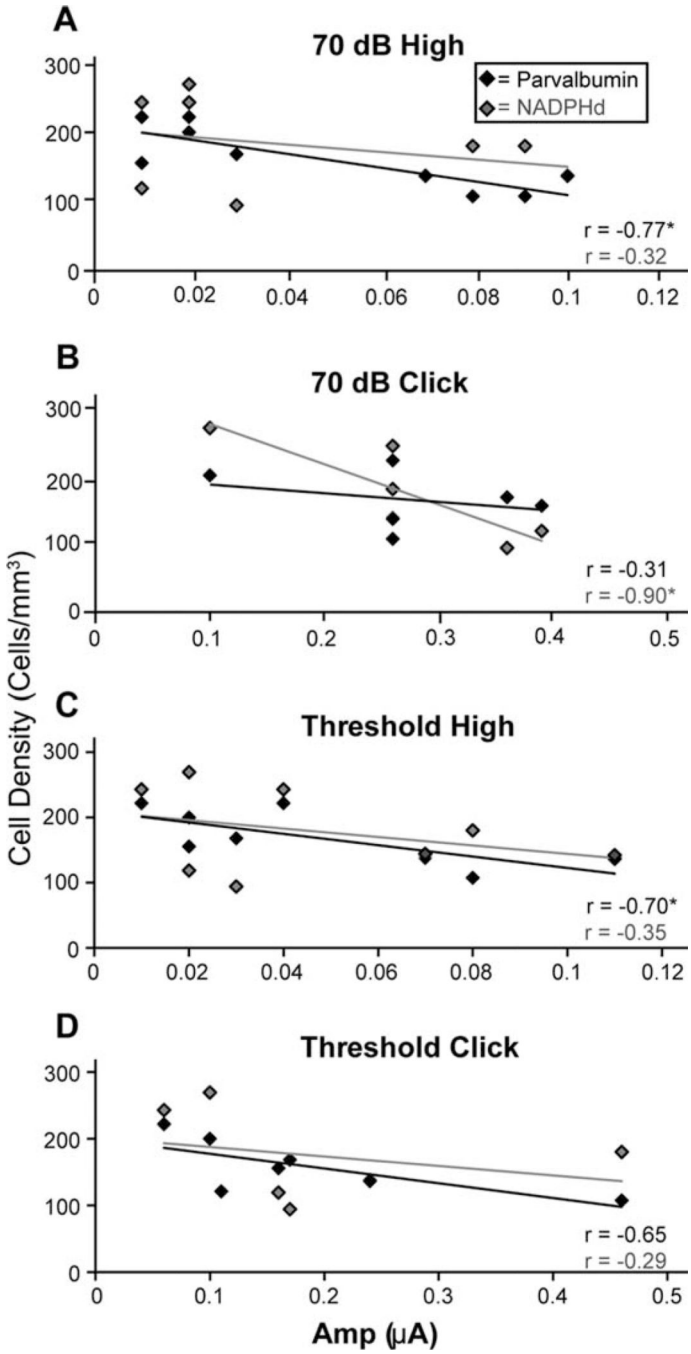

Figure 5.

The relationship between wave II auditory brainstem response (ABR) amplitudes and NADPH-diaphorase (NADPHd) and parvalbumin (PV) cell densities combined from all subdivisions of the cochlear nucleus. **A**: 70 dB high-frequency tones evoked amplitudes that significantly correlated with PV densities, but not NADPHd densities, whereas **(B)** 70 dB clicks evoked amplitudes that correlated with NADPHd but not PV. Amplitudes to threshold stimuli significantly correlated with PV densities for both **(C)** high-frequency tones and **(D)** clicks, whereas NADPHd densities did not correlate with either.

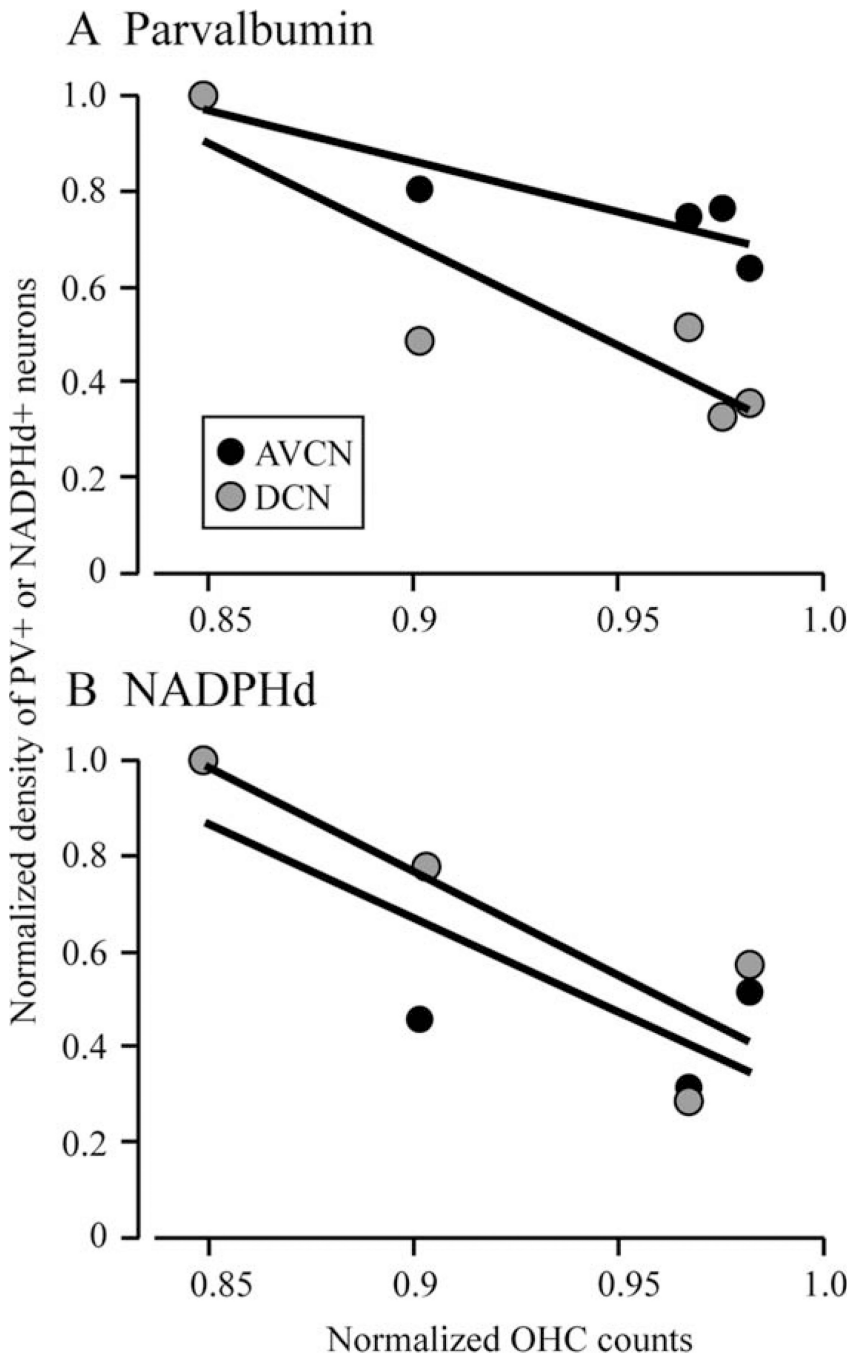

Figure 6.

The relationship between outer hair cell loss and the density of NADPHd+ and PV+ neurons. Both panels show data from the AVCN (black) and DCN (gray) symbols. Data from the PVCN showed no statistically significant trends and is not shown. **A**: Density of PV+ neurons as a function of OHC loss did reveal a statistically significant relationship in both the AVCN and the DCN. **B**: Density of NADPHd+ neurons as a function of outer hair cell loss revealed no significant correlations, although there was a relatively high regression coefficient ($r = 0.90$; $P = 0.19$; 0.94, $P = 0.15$ for AVCN and DCN, respectively). No other

cochlear histopathology correlated with either NADPHd or PV densities in any of the three CN subdivisions. All data were normalized to the greatest value from the dataset in each study.

TABLE 1

Demographics, ABR, and Anatomical Methods Used in Monkeys

Age (mo)	Human Age (yr)	Gender	ABR	Thickness (μm)	Auditory Training
147	37	Male	No	25	No
185	45	Male	Yes	30	No
243	61	Female	Yes	50	Yes
245	61	Female	Yes	40	No
267	67	Female	Yes	50	No
276	69	Female	Yes	50	No
324	81	Male	Yes	40	Yes
427	107	Female	Yes	25	No

TABLE 2

Information on the Antibodies and Chemicals Used for Immunohistochemical and Histochemical Reactions

	Antibody/Chemical	Immunogen Structure	Manufacturer/ Log #/ Other Information
Parvalbumin immunohistochemistry	Monoclonal anti-parvalbumin clone PARV-19	PARV-19 hybridoma	Sigma-Aldrich, P-3088; monoclonal; raised in mouse
Parvalbumin immunohistochemistry	Biotinylated anti-mouse IgG	Mouse IgG	Vector Labs, BA-2000; made in horse
Parvalbumin immunohistochemistry	Normal horse serum	N/A	Vector Labs, S-2000
Parvalbumin immunohistochemistry	SG- substrate kit	N/A	Vector Labs SK-4700
NADPH-diaphorase histochemistry	Nitroblue tetrazolium	N/A	Sigma-Aldrich, N-6876
NADPH-diaphorase histochemistry	β- nicotinamide adenine dinucleotide phosphate(NADPH)	N/A	Sigma-Aldrich, N-1630